ELSEVIER

WATER RESEARCH

High-performance thin-layer hydrogel composite membranes for ultrafiltration of natural organic matter

Heru Susanto[1], Mathias Ulbricht*

Lehrstuhl für Technische Chemie II, Universität Duisburg-Essen, 45117 Essen, Germany

ARTICLE INFO

ABSTRACT

Thin-layer hydrogel composite (TLHC) ultrafiltration (UF) membranes were synthesized by photo-grafting of either poly(ethylene glycol) methacrylate (PEGMA) or N,N-dimethyl-N-(2-methacryloyloxyethyl-N-(3-sulfopropyl) ammonium betaine (SPE) onto commercial polyethersulfone (PES) UF membranes. The performance of TLHC UF membranes was evaluated for natural organic matter (NOM) filtration and compared to commercial PES UF membranes. The fouling evaluation was done by investigation of membrane–solute interactions (adsorptive fouling) and membrane–solute–solute interactions (UF). The results suggest that the TLHC membranes convincingly displayed a higher adsorptive fouling resistance than unmodified PES UF membranes. In long-term stirred dead-end UF, a much lower fouling was observed for TLHC membranes than for commercial membranes with the same flux and rejection. Further, water flux recovery was also much higher. An analysis using an existing blocking model was performed in order to elucidate the effect of a polymer hydrogel layer on fouling mechanism as well as cake layer characteristics. The TLHC membranes synthesized by photo-grafting of PEGMA (40 g/L) and PEGMA with a low concentration of cross-linker monomer in the reaction mixture (ratio: 40/0.4 (g/L)/(g/L)) showed a much better performance than the other composite membranes. Those membranes could reduce the cake resistance on the membrane surface. This work has relevance for the design of high-performance UF membranes for applications in water treatment.

1. Introduction

Due to more stringent regulations with respect to water quality and environment protection on the one hand, and the decreasing quality and quantity of available water resources on the other hand, ultrafiltration (UF) has recently become an attractive technology to replace conventional water treatment processes (Glucina et al., 2000; Le-Clech et al., 2006). UF can remove not only suspended particles and microorganisms but also dissolved macromolecules such as proteins and polysaccharides. The use of UF membranes in water treatment is focused on two areas of application, namely for drinking water production and, coupled with bioreactors, for wastewater treatment. However, fouling reduces the performance as well as process economics and hence restricts a more widespread applicability of UF.

It is generally known that the natural organic matter (NOM) is considered as one of the key foulants during water treatment using membrane processes (see, e.g., Jucker and Clark, 1994; Nyström et al., 1996; Hong and Elimelech, 1997; Thorsen, 1999; Yamamura et al., 2007; Huang et al., 2007; Gray et al., 2007). In addition, NOM was also found as one of the

potential foulant components in membrane bioreactor systems for wastewater treatment (Jarusutthirak et al., 2002; Jin et al., 2004). This observation is supported by a recent study of Wang et al. (2007). They reported that the organics in the supernatant and the extracellular polymeric substances (EPS) of the bulk sludge and the cake sludge consist mainly of polysaccharides, proteins and humic acid (HA). Humic substances are a major fraction of the NOM system, and they are anionic macromolecules of low to moderate molecular weight and contain both aromatic and aliphatic components, with mainly carboxylic and phenolic groups. The content of carboxylic groups ranges from 60% to 90% of all functional groups (Aiken et al., 1985).

Membrane fouling caused by humic substances is influenced by three major factors, i.e., characteristics of both humic substance and membrane, chemical environments in the feed and hydrodynamic conditions. Hydrophilicity/phobicity, pore size, surface charge and surface roughness are the important membrane characteristics affecting the fouling behavior (Jucker and Clark, 1994; Yuan and Zydney, 2000; Schäfer et al., 1998; Lee et al., 2005; Gray et al., 2007) while the characteristics of humic substances include concentration, humic/non-humic NOM fraction ratio, molecular weight distribution and net charge (Schäfer et al., 1998; Cho et al., 2000; Nilson and DiGiano, 1996). Important feed conditions include the ionic strength, the pH and the concentration of divalent ions (mostly Ca^{2+}) (Jucker and Clark, 1994; Hong and Elimelech, 1997; Cho et al., 2000; Jones and O'Melia, 2000). Further, the transmembrane pressure and the stirring condition or cross-flow velocity are the most important of the hydrodynamic process conditions (Hong and Elimelech, 1997; Yuan and Zydney, 2000; Schäfer et al., 1998; Crozes et al., 1997; Huang et al., 2007).

Fouling studies in UF including identification/characterization of foulants, investigation of fouling mechanism and minimizing or control of fouling have been intensively performed to increase the performance of UF. Less attention compared to the other studies has been devoted to the control of fouling; however, it seems to be the most critical issue from a practical point of view. Process conditions have been remarkably engineered in order to achieve a better control of membrane fouling, but in most cases, the permeate fluxes are determined by the UF membrane itself. Therefore, low fouling UF membranes are strongly needed. Cellulose-based membranes, such as stabilized regenerated cellulose, are the state-of-the-art for low-fouling UF membranes. However, their low chemical stability and relatively low surface porosity are the significant limitations. Therefore, surface modification of established commercial membranes made of, e.g., polyethersulfone (PES) or polysulfone, while preserving their chemical resistance and mechanical strength, is of great interest for producing low-fouling UF membranes.

Recently, we have synthesized thin-layer hydrogel composite (TLHC) PES-based UF membranes by photo-graft copolymerization of water-soluble monomers, poly(ethylene glycol) methacrylate (PEGMA) and N,N-dimethyl-N-(2-methacryloyloxyethyl-N-(3-sulfopropyl) ammonium betaine (SPE), onto commercial PES UF membranes (Susanto and Ulbricht, 2007). The resulting TLHC UF membranes had a much higher protein fouling resistance than unmodified PES UF membranes having similar flux and rejection.

In this work, the performance of those TLHC UF membranes was evaluated by using solutions of another potential foulant occurring in drinking water resources and wastewater effluents. HA was used as the model of that foulant. The study was conducted by investigation of the membrane–solute and the membrane–solute–solute interactions. A classical blocking fouling model was used in order to identify the effects of a polymer hydrogel layer on the fouling mechanism whereas the cake filtration model was used to discuss the cake layer characteristics.

2. Experimental section

2.1. Materials

PES UF membranes with a nominal molecular weight cut-off (NMWCO) of 100 and 10 kg/mol provided by Sartorius AG (Göttingen, Germany) were used for modification and as reference, respectively. Prior to use for all experiments, the membranes were washed with ethanol by shaking at 100 rpm on a mechanical shaker for 1.5–2 h and then equilibrated with water. Only membrane samples that had initial water permeability in the range ±15% relative to the average values were used (see Susanto and Ulbricht (2005) for this selection procedure). PEGMA 400 (the number indicating molar mass of the PEG in g/mol) and SPE 279 (the number indicating molar mass of the monomer in g/mol) were from Polysciences Inc. (Warrington, USA) and Raschig GmbH (Germany), respectively. Hydrophilic cross-linker monomer, N,N'-methylenbisacrylamide (MBAA), and HA were purchased from Sigma-Aldrich Chemie GmbH (Steinheim, Germany). Nitrogen gas purchased from Messer Griesheim GmbH (Krefeld, Germany) was of ultrahigh purity. Water purified with a Milli-Q system from Millipore was used for all experiments.

2.2. Membrane modification and characterization

The method and experimental setup used for modification have already been described in detail (Susanto and Ulbricht, 2007). Briefly, a UVA Print system (Hoenle AG, Gräfelfing, Germany) equipped with a high-pressure mercury lamp, emitting wavelengths > 300 nm and providing homogeneous illumination of up to 100 cm^2 area with an intensity of 35 ± 5 mW/cm^2, was used. PES membrane samples were immersed into monomer solutions in a Petri dish. A second smaller glass Petri dish was used to cover the membranes and also as another deep-UV filter. The samples were then subjected to UV irradiation for various time periods. Thereafter, the membranes were taken out, immediately rinsed with water and then washed with excess of water to remove any unreacted monomer or physically adsorbed polymer.

Membrane characterization by contact angle (CA) and zeta potential measurements have been performed as described before (Susanto and Ulbricht, 2007).

2.3. Static adsorption, ultrafiltration procedure and solute analysis

Solid-state NMR spectra of HA were recorded using an instrument DRX 500 (Bruker). Membrane experiments were performed using a dead-end stirred cell filtration system consisting of a filtration cell (Amicon model 8010, Millipore) connected to a reservoir. It was pressurized by nitrogen. To avoid the effects of membrane compaction on the interpretation of modification and fouling data, each sample was firstly compacted by filtration of pure water at a pressure of 450 kPa for at least 0.5 h. Thereafter, the pressure was reduced to the desired pressure for water flux measurement. For static adsorption experiments, the water flux was initially measured and then a HA solution was added to the cell. The outer membrane surface was exposed for 18 h without any flux through the membrane at a stirring rate of 300 rpm (a preliminary adsorption kinetics study had shown that 18 h was sufficient to achieve saturation of the surface adsorption capacity for this HA). Then, the HA solution was removed and the membrane surface was cleaned two times by filling the cell with pure water (5 mL) and shaking it for 30 s. Water fluxes before and after exposing were compared. The evaluation of membrane performance was expressed in terms of relative water flux reduction, RFR (cf. Eq. (1)):

$$RFR = \frac{J_o - J_{ads}}{J_o} \qquad (1)$$

where J_o and J_{ads} are water flux before and after exposing to the HA test solution, respectively. UF experiments were carried out at constant transmembrane pressure with identical initial water flux for all membranes. In these experiments, the balance was connected to the PC, the weight of permeate was online recorded and the flux was calculated. HA concentrations were determined by measuring UV absorbance at 255 nm. Profiles of permeate fluxes and apparent solute rejections over time were obtained. All experiments were performed at room temperature (21 ± 1 °C). Cleaning of the membranes after UF was done, with the sample still in the filtration cell but with closed permeate line, using pure water (shaking at 300 rpm and 21 ± 1 °C for 15 min). Pure water flux was measured thereafter. Then samples were dried in an oven at 45 °C, and the deposited mass of HA was determined gravimetrically (balance Genius, Sartorius) and expressed relative to the outer surface area of the samples.

3. Results and discussion

3.1. TLHC UF membrane characteristics

As mentioned above, the performance of an UF process is very much influenced by the membrane characteristics as well as solute/particle characteristics. Table 1 presents the characteristics of the membranes used in this study. It is important to mention that the grafted polymer was covalently attached on the PES base membrane (Susanto and Ulbricht, 2007). This grafted polymer changed significantly the membrane characteristics of the base membrane (PES-SG100). TLHC membranes had much smaller water permeability than the base membrane, but values were similar to a commercial PES membrane having a nominal cut-off of 10 kg/mol (PES-SG10). They had slightly larger

Membranes	Code	Water permeability[a] (L/m^2 h kPa)	Contact angle[b] (deg)	Nominal cut-off[c] (kg/mol)	Zeta potential[d] at pH 8/3.5 (mV)
PES-SG10 (unmodified)	PES-SG10	0.90	61.7	8.0	−24.8/−10.8
PES-SG100 (unmodified)	PES-SG100	5.71	44.8	89.9	−20.4/−9.4
PES-g-polyPEGMA (40[e],0[f],5[g])	TLHC1	1.29	39.8	10.4	−9.5/−5.3
PES-g-polyPEGMA/MBAA (40[e], 0.4[f],5[g])	TLHC2	0.84	41.1	10.1	n.d.
PES-g-polyPEGMA/MBAA (40[e],2[f],4[g])	TLHC3	1.19	42.1	10.6	−10.8/−6.5
PES-g-polySPE (40[e],0[f],6[g])	TLHC4	0.77	44.5	10.4	−8.2/−4.2
PES-g-polySPE/MBAA (40[e],2[f],5[g])	TLHC5	0.85	45.3	9.8	−13.6/−5.8

Table 1 – Characteristics of the unmodified and TLHC UF membranes used in this study

n.d.: not done.
[a] Determined using a dead-end stirred filtration at a temperature of 21 ± 1 °C.
[b] Measured using the captive bubble method.
[c] Determined with a PEG mixture at a total concentration of 1 g/L at constant transmembrane pressure (100 kPa).
[d] Measured at a temperature of 25 ± 1 °C.
[e] Functional monomer concentration (g/L).
[f] Cross-linker monomer concentration (g/L).
[g] UV irradiation time (min).

nominal cut-off than PES-SG10. More importantly, all TLHC UF membranes had much lower CA than PES-SG10, indicating a more hydrophilic surface. It is also important to note that the CA data of the TLHC UF membranes should not directly be compared to those of the base membrane, PES-SG100, because the membranes have different pore size and surface porosity. These TLHC UF membranes were much less negatively charged compared to PES unmodified membranes as noticed by their lower (absolute) zeta potential, indicating that these membranes were less prone to anion adsorption than unmodified membranes (cf. Susanto and Ulbricht (2007) for more details on modified membrane characteristics).

3.2.   Humic acid characteristics

One of the major limitations when working with commercial HAs is their variation in properties (Malcolm and MacCarthy, 1986). Consequently, results obtained from one case cannot immediately be applied for other cases with different humic substance. Therefore, in this work, the HA was firstly characterized. Fig. 1 shows the NMR spectrum of the HA used. It is observed that the HA is mainly composed of aliphatic and aromatic groups as evidenced by the appearance of peaks in the ranges 0–50 and 108–145 ppm, respectively. In addition, carbohydrate and aromatic C–O were also observed in the ranges of 60–96 and 145–162 ppm, respectively. This indicates that the HA consisted of both more hydrophilic and more hydrophobic moieties. However, the content of more hydrophilic moieties (e.g., phenolic groups) was much larger than the hydrophobic fraction. Overall, even though the heterogeneity of HA is a common problem, this result agrees well with previous results reported by Mao et al. (2002).

3.3.   Adsorptive fouling (membrane–solute interactions) performance test

In many cases, adsorptive fouling determines the total fouling in UF membranes (e.g., (Matthiasson, 1983; Susanto and Ulbricht, 2005). The resistance of TLHC UF membranes towards adsorptive fouling of HA was investigated at various pH values. In addition, calcium ions (1 mM) were added and the ionic strength was increased (conductivity 1100 μS/cm) in order to obtain severe fouling. The addition of calcium ions was performed only at neutral pH because many other groups had already studied the effect of calcium ion at different pH (cf. below). The fouling resistance was observed in terms of relative water flux reduction (RFR).

The results in Fig. 2 show that exposing the membrane to the HA solutions reduced the water flux. As also found in the previously reported literature (Jucker and Clark, 1994; Hong and Elimelech, 1997; Jones and O'Melia, 2000; Mänttäri et al., 2000), fouling was larger in the acidic pH range than in the alkaline one. It is important to note that an increase of water flux after exposing to the alkaline HA solution was observed in the beginning of the water flux measurements. This phenomenon might be one of the reasons for previous disagreements among different authors in the interpretation of the effect of adsorptive fouling on RFR under alkaline conditions. The larger adsorptive fouling at lower pH is attributed to the more compact character and more hydrophobic structure of HA in water under those conditions, and this can be related to the protonation of the carboxylic groups. It should be noted that at low pH, the surface charge of the TLHC membrane was close to neutral (cf. Table 1). Therefore, electrostatic interactions should not be involved or at least minimal. Interestingly, all TLHC membranes showed significantly lower RFR than unmodified membranes with similar cut-off (PES-SG10) and also when compared to the base membrane (PES-SG100; except for TLHC4/PES-g-poly-SPE). This observation indicates that the (adsorptive) fouling resistance of composite membranes was stronger than of unmodified PES membranes. Further analysis shows that there was a correlation between RFR and CA, especially for membranes having similar cut-off (Fig. 3). This implies that hydrophilization by hydrogel polymer is quite effective to minimize NOM fouling. It is also seen in Fig. 2 that membrane
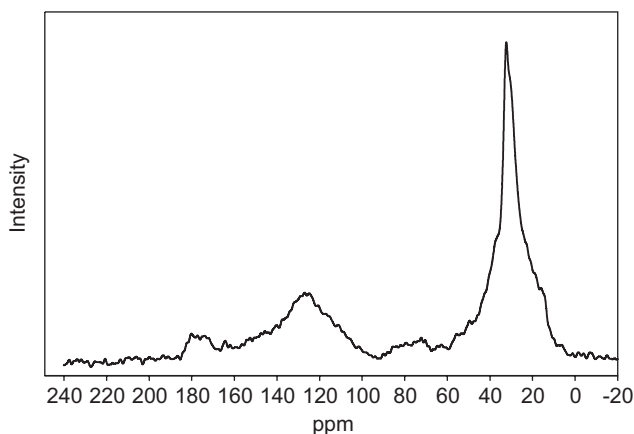

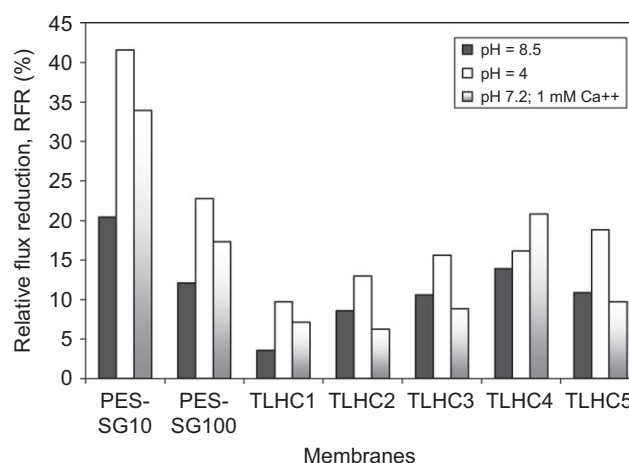Fig. 1 – CP MAS ^{13}C NMR spectra of humic acid used.

Fig. 2 – RFR of unmodified PES and TLHC UF membranes after static adsorption (18 h) of HA solutions (100 mg/L) at various pH values. PES-SG10 and PES-SG100 are unmodified membranes with nominal cut-offs of 10 and 100 kg/mol, respectively.
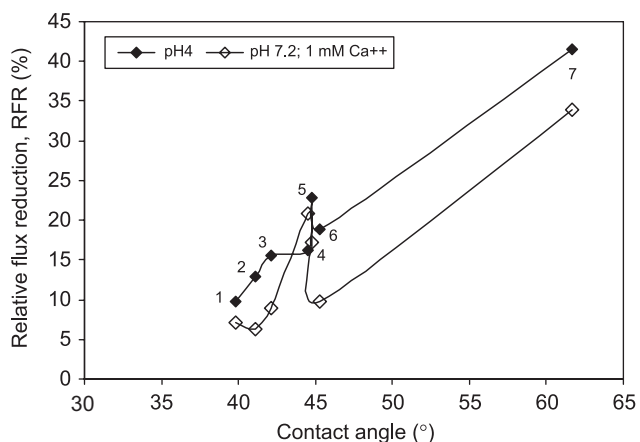
Fig. 3 – **Correlation between RFR and membrane contact angle: (1) TLHC1, (2) TLHC2, (3) TLHC3, (4) TLHC4, (5) PES-SG 100, (6) TLHC5 and (7) PES-SG10.**
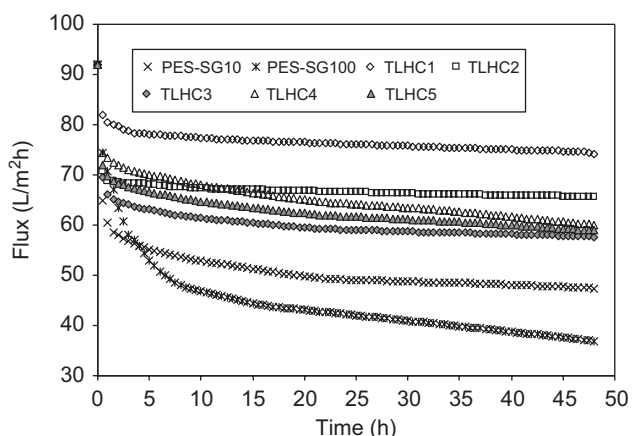

Fig. 4 – **Flux profile as a function of time during ultrafiltration of humic acid (50 mg/L, pH 7.2, 1 mM Ca^{2+}, conductivity 1100 μS/cm) at similar initial water flux (~92 L/m^2 h).**

pore size influenced the extent of adsorptive fouling, i.e., membranes with smaller pore size showed higher adsorptive fouling as evidenced by its higher RFR. Apparently, the pore blocking was more severe for membranes with smaller pores. It should be noted that the pore blocking will yield a higher contribution to membrane resistance than pore narrowing (Belfort et al., 1994). However, this result is in contrast to the result of the UF experiments (cf. Fig. 4).

3.4. Ultrafiltration (membrane–solute–solute interactions) performance test

UF has been performed in order to know the performance of the TLHC UF membranes from the application point of view. The experiments were performed by using the feed with addition of calcium ions and at high ionic strength to obtain high fouling. The evaluation was expressed in terms of permeate flux profile and HA rejection over filtration time. Again, the unmodified PES-SG10 was also included to consider the effect of flux rejection trade-off (Fig. 4).

As presented in Fig. 4, it is obviously seen that all composite membranes had higher permeate fluxes than both unmodified membranes. For example, the PES-g-polyPEGMA (TLHC1) and PES-g-polyPEGMA/MBAA (TLHC2), which had similar rejection curve and cut-off with unmodified PES-SG10 (see Susanto and Ulbricht (2007) for more details), showed permeate fluxes of approximately 80% and 72%, respectively, relative to their initial water flux. By contrast, the unmodified membranes PES-SG10 and PES-SG 100 showed permeate fluxes of only approximately 51% and 39%, respectively, of their initial water flux. Even though UF has been done at similar initial water flux (i.e., ~92 L/m^2 h) in order to minimize effects of hydrodynamic conditions, membranes with larger pore sizes showed more severe fouling (cf. PES-SG10 vs. PES-SG100). This phenomenon is likely due to the higher accessibility of the membrane pores to the HA colloids. As a result, fouling occurred not only on the outer membrane surface but also within the membrane pores. This result agrees well with other reported studies (Cho et al., 2000; Costa and de Pinho, 2005). However, this is in contrast with the results of adsorptive fouling (cf. above), indicating that the hydrodynamic conditions significantly contributed to the fouling behavior. Such different behavior between adsorptive fouling and UF fouling with respect to the effect of pore size had been well explained earlier (Ko et al., 1993). Here it was also observed that solute–solute interactions play an important role during UF experiments (see fouling mechanism below in more detail).

The apparent rejections of TLHC UF membranes were similar to those for the unmodified membrane having identical molecular weight cut-off (i.e., ~91–95%, Table 2). More importantly, it is also observed that the water fluxes after external cleaning (with shaking) were significantly higher for the TLHC membranes than for the unmodified membranes (cf. Table 2). This cleaning process could recover the initial water fluxes to approximately 90% and 86% for PES-g-polyPEGMA and PES-g-polyPEGMA/MBAA, respectively. By contrast, the same cleaning procedure conducted for unmodified membranes yielded ~65% and ~47% recovery for PES-SG10 and PES-SG100, respectively. These results indicate that a different foulant layer was attached on/in the TLHC and the unmodified PES membranes (cf. below in more detail).

3.5. Effect of polymer hydrogel layer on fouling mechanism

The effect of modification on fouling mechanism behavior was studied by using the following "standard" classical blocking model proposed by Hermia (1982):

$$\frac{d^2t}{dV^2} = k\left(\frac{dt}{dV}\right)^n \tag{2}$$

where t is the filtration time, V is total filtered volume, k is a fouling coefficient and n is a dimensionless filtration constant reflecting the mode of fouling. That model describes three possible fouling mechanisms, i.e., pore blocking, pore constriction and cake formation. Cake formation corresponds to the value of $n = 0$, whereas complete pore blocking

Table 2 – Initial water flux, permeate flux, water flux after external cleaning[a] and apparent humic acid rejection during ultrafiltration

No.	Membrane	TMP (kPa)	Initial water flux (L/m²h)	Permeate flux at 48 h (L/m²h)	Water flux after cleaning (L/m²h)[a]	HA rejection (%)[b]
1	PES-SG10 (unmodified)	90	91.7	47.3	59.2	95.4±2.1
2	PES-SG100 (unmodified)	15	93.6	37.0	44.2	86.5±3.1
3	TLHC1	60	92.5	74.1	83.3	91.5±2.3
4	TLHC2	95	91.6	65.6	78.9	92.3±2.4
5	TLHC3	70	91.0	57.6	72.2	93.1±2.5
6	TLHC4	110	92.0	60.1	70.3	93.3±2.6
7	TLHC5	95	93.1	58.9	75.2	94.1±2.4

[a] Membrane was externally cleaned using pure water and shaking.
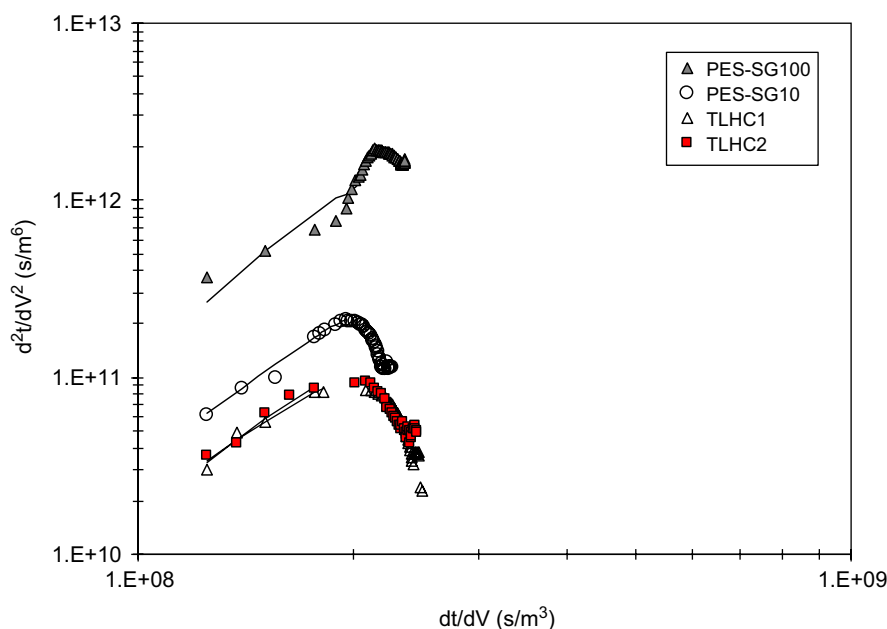[b] Average value from time filtration of 12, 24, 36 and 48 h.

Fig. 5 – NOM fouling mechanism analysis according to standard blocking model (cf. Eq (2)) for unmodified and TLHC UF membranes.

corresponds to $n = 2$. Pore constriction (standard blocking) is represented by the value of $n = 3/2$ (cf. (Hermia, 1982; Ho and Zydney, 2000) for more details). This blocking model had also been used to analyze the fouling mechanism during NOM UF by previous authors (Costa et al., 2006; Taniguchi et al., 2003).

The filtrate flux over time data (Fig. 3) were plotted as d^2t/dV^2 versus dt/dV as described by Eq. (2). The required derivatives were evaluated in terms of the filtrate flux (Eqs. (3) and (4); Ho and Zydney, 2000):

$$\frac{dt}{dV} = \frac{1}{JA} \qquad (3)$$

$$\frac{d^2t}{dV^2} = -\frac{1}{J^3A^2}\frac{dJ}{dt} \qquad (4)$$

dJ/dt was evaluated by differentiating the adjusting polynomials that gave the best fit of the experimental data in Fig. 4.

Fig. 5 shows the analysis of flux decline for both unmodified and the two PEGMA-based TLHC UF membranes. In general, a similar fouling mechanism was observed for both TLHC membranes and the PES-SG10 membrane: At the beginning of filtration, which corresponds to small dt/dV values, involving all data before reaching the cake formation regime ($n = 0$) yielded a slope (n) greater than 2, i.e., $n = 2.4$, 2.3 and 2.4 for PES-SG10, TLHC1 and TLHC2, respectively (obviously, the resulting n value will depend on the number of data included). This phenomenon could not quantitatively be explained by this "standard" classical model. However, it is still reasonable to discuss the fouling mechanism using this model qualitatively, i.e., pore narrowing and pore blocking

seemed to occur. A similar observation ($n > 2$) was also made by Ho and Zydney (2001) during protein filtration using asymmetric and composite membranes. At long filtration times, the mechanism changed to the classical cake filtration model as noticed by the fact that n is equal to zero. A slightly different mechanism was observed for the PES-SG100 membrane for short filtration times (i.e., before reaching the regime with $n = 0$), as evidenced by the different slope of the curve. This indicates that the contributions of pore constriction and complete pore blocking were different from the behavior of the PES-SG10 and the TLHC UF membranes, all having smaller average pore sizes.

Comparing the PES-SG10 and TLHC UF membranes in detail reveals two interesting phenomena caused by the modification with the grafted polyPEGMA hydrogel, i.e., (i) the maximum value in the plot of d^2t/dV^2 versus dt/dV was reduced and (ii) the change in n value to $n = 0$ was reached at almost similar values, i.e., at $dt/dV = 2 \times 10^8$, 1.8×10^8 and 2×10^8 for PES-SG 10, TLHC 1 and TLHC 2, respectively. The first observation indicates that the amount of accumulated NOM particles as a potential cause of the cake resistance on the TLHC membranes was less than that on the unmodified PES-SG10 membrane. This explanation is supported by the results obtained from investigations of specific cake resistance (cf. Section 3.6). Ho and Zydney (2000) reported that during UF of protein, the maximum value of d^2t/dV^2 increased with increasing bulk protein concentration. The latter observation shows that the transition of fouling mechanism to cake filtration occurred at a similar filtration time for TLHC membranes and unmodified membranes. Further, this indicates that there is no effect of modification on the fouling mechanism transition mechanism to cake filtration. No significant difference was observed between the TLHC membranes synthesized without and with cross-linker monomer at low content (the effect of cross-linker on membrane separation characteristic had been analyzed previously (Susanto and Ulbricht, 2007)).

3.6. Effect of polymer hydrogel layer on cake layer characteristics

The effect of modification on the characteristics of the fouling layer was also investigated. Fig. 6 shows the photographs of the membrane surfaces taken after external cleaning. Significant differences in fouling layer structure were observed between the unmodified and the TLHC membranes, and even among the different TLHC membranes. No significant difference in appearance of the cake layer before and after cleaning was observed for both unmodified membranes. By contrast, significant HA layer removal from the membrane surface was observed for TLCH1 (PES-g-polyPEGMA) and TLCH2 (PES-g-polyPEGMA/MBAA) membranes, indicating that the membrane–foulant interactions were weak and could be easily overcome by simple washing. This result is in good agreement with the measured water flux recovery by external washing (cf. Table 2). Nevertheless, not all photographs correlated with the permeate flux behavior as well as the water flux recovery. For example, even though the photograph of the TLHC4 (PES-g-polySPE) membrane indicates that the attachment of the fouling layer
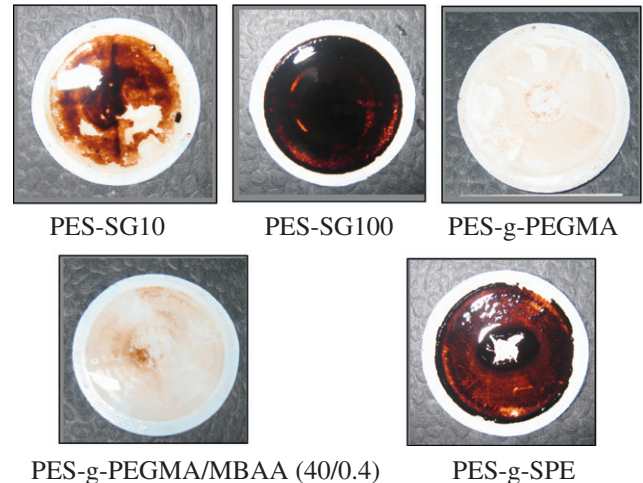

PES-SG10   PES-SG100   PES-g-PEGMA

PES-g-PEGMA/MBAA (40/0.4)   PES-g-SPE

Fig. 6 – Photographs of the fouled membrane after external cleaning with water for unmodified and TLHC UF membranes (TLHC1, 2 and 4).

seemed to be stronger than on the unmodified PES-SG10 membrane, the permeate flux during HA filtration and the flux recovery were higher values than for the PES-SG10 membrane (cf. Fig. 4 and Table 2).

An alternative approach to evaluate the fouling layer characteristics was done by applying the resistance in series model for UF membranes containing a deposited layer, as also performed by other authors (Eq. (5); Costa et al., 2006; Waite et al., 1999):

$$J = \frac{\Delta P}{\mu(R_m + R_c)} = \frac{\Delta P}{\mu R_t} \tag{5}$$

where J is the flux, ΔP is the transmembrane pressure, μ is the solution viscosity and R_t, R_m and R_c are the total, membrane and cake resistances, respectively. It should be noted that $R_t = R_m + R_c$. The membrane resistance was obtained from pure water flux measurement with $R_m = \Delta P/J\mu$. The pure water flux was measured again after filtration in order to determine the cake resistance. The specific cake resistance (α) is determined according to the following equation (Eq. (6); Costa et al., 2006; Waite et al., 1999):

$$\alpha = R_c \frac{A_m}{m_{dep}} \tag{6}$$

with A_m being membrane surface area and m_{dep} the mass deposited on and in the membrane.

As presented in Table 3, the membrane with larger pore sizes (PES-SG100) showed a lower membrane resistance (R_m) than PES-SG10. The membrane resistance for the TLCH membranes is to a large extent due to the added resistance of the thin grafted polymer layer on the base membrane (PES-SG100). We had observed that linear grafted polyPEGMA is more swollen than linear grafted polySPE (Susanto and Ulbricht, 2007); consequently the former (in TLHC1) provides a lower added resistance (than in TLHC4). Cross-linking increased resistance for polyPEGMA (but in a more complex manner, i.e., largest effects for small content of cross-linker

Table 3 – Transmembrane pressure, deposited mass of foulant (from gravimetry) and characteristics of the fouling layer according to resistance in series model							
Membrane	TMP (kPa)	m_{dep} (g/m²)	R_m (10^{12} m⁻¹)	R_t (10^{12} m⁻¹)	R_c (10^{12} m⁻¹)	R_c/R_t	α (10^{11} m/g)
PES-SG10	90	11.84	3.53	5.47	1.93	0.35	1.634
PES-SG100	15	27.25	0.58	1.22	0.64	0.53	0.236
TLHC1	60	2.24	2.34	2.59	0.26	0.10	1.152
TLHC2	95	2.91	3.74	4.34	0.60	0.14	2.069
TLHC3	70	9.00	2.77	3.49	0.72	0.21	0.798
TLHC4	110	18.81	4.30	5.63	1.33	0.24	0.708
TLHC5	95	4.20	3.67	4.55	0.88	0.19	2.089

monomer; in TLHC2) while the influence for polySPE was smaller (because overall degree of swelling is lower). Interestingly, the TLHC1 had a lower membrane resistance compared to the commercial membrane having a similar rejection curve and cut-off (PES-SG10).

The mass deposited on the membrane surface after UF (less for TLHC1 than for TLHC4; cf. Table 3) seemed to correlate with the intrinsic fouling resistance of the grafted polymer layer (grafted polyPEGMA had larger fouling resistance than grafted polySPE; Susanto and Ulbricht, 2007). Most TLHC membranes had a lower mass deposited than PES-SG10; the larger mass deposited for TLHC4 compared to unmodified PES-SG10 was surprising. Membrane fouling resistance could be improved by cross-linking (as is the case for SPE; see TLHC4 vs. TLHC5), but too large a degree of cross-linking reduced the fouling resistance (see TLHC3 vs. TLHC 2 and TLHC1; cf. Susanto and Ulbricht, 2007).

The R_c/R_t ratio is a measure of cake layer fouling propensity during UF, but this measure is influenced by the membrane, the structure of the cake layer and the UF conditions. Interestingly, all TLHC membranes (even TLHC4) showed a smaller R_c/R_t ratio than the unmodified PES-SG10 membrane (cf. Table 3). It can be assumed that under the experimental conditions, the influence of different pressure onto the structure of the cake layer is negligible. Instead, by setting the same initial flux and considering that all membranes had similar rejection for HA, similar conditions of the formation of the fouling layer could be provided. However, this fouling layer was presumably not homogeneous: The interface of this cake layer to the membrane surface may have a pronounced effect on its resistance (the better the "drainage", the lower this interface resistance), and the cake layer density may decrease with distance to the membrane surface.

Consequently, the lowest value of specific cake resistance (α) was found for the membrane PES-SG100 with large pore size (lower pore size PES-SG10 has worse "drainage" for the fouling layer; cf. Table 3). Rather low α values were also found for the two composite membranes (TLHC3 and TLHC4) with largest deposited masses (i.e., more foulant remote from membrane surface and hence at lower density). Among the other three composite membranes, TLHC1 had by far the lowest α value, and this is explained by the highest degree of swelling of the grafted layer (providing better "drainage" than a more cross-linked PEGMA- or a less swelling SPE-based layer as in TLHC2 and TLHC5, respectively).

4.   Conclusion

Overall, the anti-fouling properties of PES-based composite membranes for UF have been convincingly demonstrated, and they are clearly related to the hydrogel structure of the thin grafted polymer layer on the outer membrane surface. Irrespective of the almost identical membrane characteristics (cf. Table 1), the TLHC membranes synthesized using an established PEG-containing monomer (TLHC1 and 2) were clearly superior to those obtained using an alternative zwitterionic monomer (TLHC4 and 5). These differences may be explained by the lower degree of swelling of the SPE- compared to the PEGMA-based polymer hydrogels (Susanto and Ulbricht, 2007). Slight chemical cross-linking of the polymer hydrogels layer, here by using a hydrophilic cross-linker monomer, can be used to improve the antifouling performance (TLHC5 vs. TLHC4), but at too high a degree of cross-linking the performance is significantly reduced (TLHC3 vs. TLHC2). The anti-fouling mechanism imparted by the thin grafted interlayer is due to the reduction of the adsorption tendency of solute on the PES surface (adsorption experiments and early stage of UF), and the prevention of a tight adhesion of the foulant cake layer on the PES membrane surface (later stage of UF and external cleaning). This work has relevance for the design of high-performance UF membranes for applications in water treatment, and the preparation of the tailored thin-layer composite structures could also be achieved by other preparation methods (Ulbricht, 2006).

REFERENCES

Aiken, G.R., McKnight, D.M., Wershaw, R.I., MacCarthy, P., 1985. Humic Substances in Soil, Sediment and Water: Geochemistry, Isolation, and Characteristic. Wiley, New York.

Belfort, G., Davis, R.H., Zydney, A.L., 1994. The behavior of suspensions and macromolecular solutions in crossflow microfiltration. J. Membr. Sci. 96, 1.

Cho, J., Amy, G., Pellegrino, J., 2000. Membrane filtration of natural organic matter: factors and mechanisms affecting rejection and flux decline with charged ultrafiltration (UF) membrane. J. Membr. Sci. 164, 89.

Costa, A.R., de Pinho, M.N., 2005. Effect of membrane pore size and solution chemistry on the ultrafiltration of humic substances solutions. J. Membr. Sci. 255, 49.

Costa, A.R., de Pinho, M.N., Elimelech, M., 2006. Mechanism of colloidal natural organic matter in ultrafiltration. J. Membr. Sci. 281, 716.

Crozes, G.F., Jacangelo, J.G., Anselme, C., Laîné, J.M., 1997. Impact of ultrafiltration operating conditions on membrane irreversible fouling. J. Membr. Sci. 124, 63.

Glucina, K., Alvarez, A., Laîné, J.M., 2000. Assessment of an integrated membrane system for surface water treatment. Desalination 132, 73.

Gray, S.R., Ritchie, C.B., Tran, T., Bolto, B.A., 2007. Effect of NOM characteristics and membrane type on microfiltration performance. Water Res. 41, 3833.

Hermia, 1982. Constant pressure blocking filtration laws—application to power law non-Newtonian fluids. Trans. Inst. Chem. Eng. 60, 183.

Ho, C.C., Zydney, A.L., 2000. A combined pore blockage and cake filtration model for protein fouling during microfiltration. J. Colloid Interface Sci. 232, 389.

Ho, C.C., Zydney, A.L., 2001. Protein fouling of asymmetric and composite microfiltration membranes. Ind. Eng. Chem. Res. 40, 1412.

Hong, S., Elimelech, M., 1997. Chemical and physical aspect of natural organic matter (NOM) fouling of nanofiltration membranes. J. Membr. Sci. 132, 159.

Huang, H., Lee, N.H., Young, T., Amy, G., Lozier, J.C., Jacangelo, J.G., 2007. Natural organic matter fouling of low-pressure, hollow-fiber membranes: effects of NOM source and hydrodynamic conditions. Water Res. 41, 3823.

Jarusutthirak, C., Amy, G., Croué, J.P., 2002. Fouling characteristics of wastewater effluent organic matter (EfOM) isolates on NF and UF membranes. Desalination 145, 247.

Jin, B., Wilén, B.M., Lant, P., 2004. Impacts of morphological, physical and chemical properties of sludge flocks on dewaterability of activated sludge. Chem. Eng. J. 98, 115.

Jones, K.L., O'Melia, C.R., 2000. Protein and humic adsorption onto hydrophilic membrane surfaces: effect of pH and ionic strength. J. Membr. Sci. 165, 31.

Jucker, C., Clark, M.M., 1994. Adsorption of aquatic humic substances on hydrophobic ultrafiltration membranes. J. Membr. Sci. 97, 37.

Ko, M.K., Pellegrino, J.J., Nassimbene, R., Marko, P., 1993. Characterization of the adsorption-fouling layer using globular proteins on ultrafiltration membranes. J Membr. Sci. 76, 101.

Le-Clech, P., Chen, V., Fane, A.G., 2006. Fouling in membrane bioreactors used in wastewater treatment. J. Membr. Sci. 284, 17.

Lee, N., Amy, G., Croué, J.P., Buisson, H., 2005. Morphological analyses of natural organic matter (NOM) fouling of low-pressure membranes (MF/UF). J. Membr. Sci. 261, 7.

Malcolm, R.L., MacCarthy, P., 1986. Limitation in the use of commercial humic acids in water and soil research. Environ. Sci. Technol. 20, 904.

Mänttäri, M., Puro, L., Nuortila-Jokinen, J., Nyström, M., 2000. Fouling effects of polysaccharides and humic acid in nanofiltration. J. Membr. Sci. 165, 1.

Mao, J., Hu, W., Ding, G., Schmidt-Rohr, K., Davies, G., Ghabbour, E.A., Xing, B., 2002. Suitability of different ^{13}C solid-state NMR techniques in the characterization of humic acids. Int. J. Environ. Anal. Chem. 82, 183.

Matthiasson, E., 1983. The role of macromolecular adsorption in fouling of ultrafiltration membranes. J. Membr. Sci. 16, 23.

Nilson, J.A., DiGiano, F.A., 1996. Influence of NOM composition on nanofiltration. J. Am. Water Works Assoc. 88 (5), 53.

Nyström, M., Ruohomäki, K., Kaipia, L., 1996. Humic acid as a fouling agent in filtration. Desalination 106, 79.

Schäfer, A.I., Fane, A.G., Waite, T.D., 1998. Nanofiltration of natural organic matter: removal, fouling and the influence of multivalent ions. Desalination 18, 109.

Susanto, H., Ulbricht, M., 2005. Influence of ultrafiltration membrane characteristics on adsorptive fouling with dextrans. J. Membr. Sci. 266, 132.

Susanto, H., Ulbricht, M., 2007. Photo-grafted thin polymer hydrogel layers on PES ultrafiltration membranes: characterization, stability and influence on separation performance. Langmuir 23, 7818.

Taniguchi, M., Kilduff, J.E., Belfort, G., 2003. Modes of natural organic matter fouling during ultrafiltration. Environ. Sci. Technol. 37, 1676.

Thorsen, T., 1999. Membrane filtration of humic substances—state of the art. Water Sci. Technol. 40 (9), 105.

Ulbricht, M., 2006. Advanced functional polymer membranes. Polymer 47, 2217.

Waite, T.D., Schäfer, A.I., Fane, A.G., Heuer, A., 1999. Colloidal fouling of ultrafiltration membranes: impact of aggregate structure and size. J. Colloid Interface Sci. 212, 264.

Wang, X.M., Li, X.Y., Huang, X., 2007. Membrane fouling in a submerged membrane bioreactor (SMBR): characterisation of the sludge cake and its high filtration resistance. Sep. Purif. Technol. 52, 439.

Yamamura, H., Chae, S., Kimura, K., Watanabe, Y., 2007. Transition in fouling mechanism in microfiltration of a surface water. Water Res. 41, 3812.

Yuan, W., Zydney, A.L., 2000. Humic acid fouling during ultrafiltration. Environ. Sci. Technol. 34, 5043.